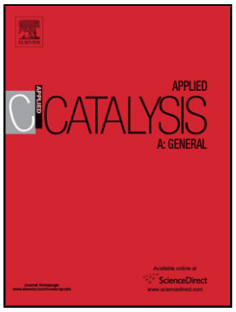

Title: CoMoW sulfide nanocatalysts for the HDS of DBT from
novel ammonium and alkyltrimethylammonium-
thiomolybdate-thiotungstate-cobaltate (II)
precursors

Author: Y. Espinoza-Armenta J. Cruz-Reyes F.
Paraguay-Delgado M. Del Valle G. Alonso S. Fuentes R.
Romero-Rivera

PII: S0926-860X(14)00502-X
DOI: http://dx.doi.org/doi:10.1016/j.apcata.2014.08.017
Reference: APCATA 14954

To appear in: *Applied Catalysis A: General*

Received date: 7-6-2014
Revised date: 12-8-2014
Accepted date: 18-8-2014

Please cite this article as: Y. Espinoza-Armenta, J. Cruz-Reyes, F. Paraguay-Delgado, M. Del Valle, G. Alonso, S. Fuentes, R. Romero-Rivera, CoMoW sulfide nanocatalysts for the HDS of DBT from novel ammonium and alkyltrimethylammonium-thiomolybdate-thiotungstate-cobaltate (II) precursors, *Applied Catalysis A, General* (2014), http://dx.doi.org/10.1016/j.apcata.2014.08.017

GRAPHICAL ABSTRACT

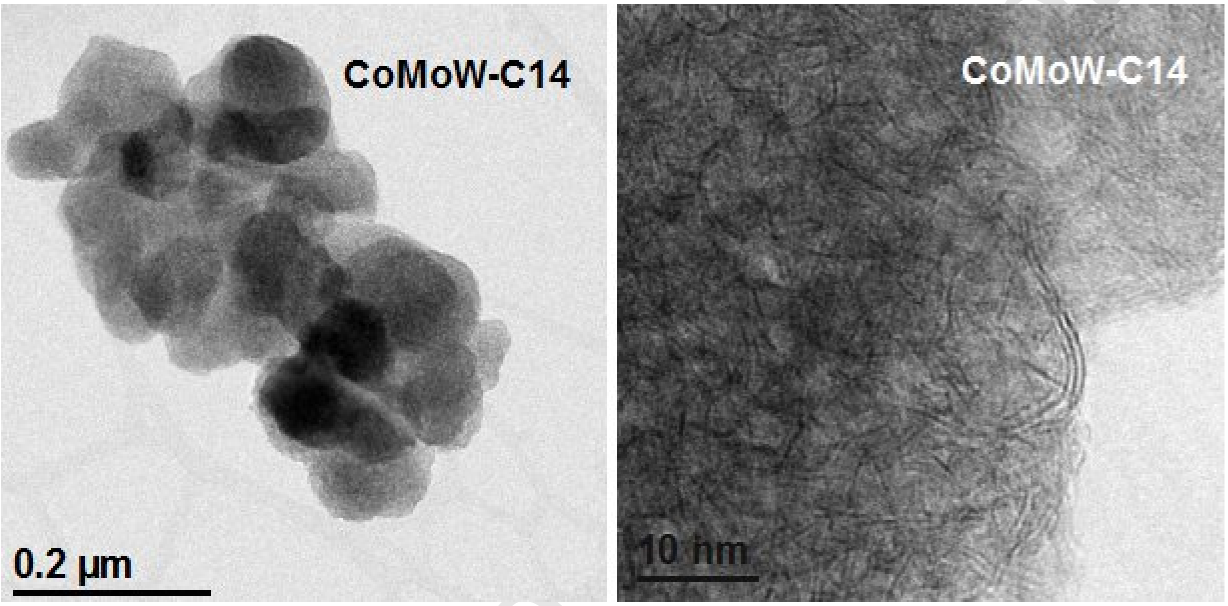

HIGHLIGHTS

- Highly active CoMoW nanocatalysts were obtained from novel precursors.
- These nanocatalysts are mesoporous materials with surface areas up to 340 m^2/g.
- XRD and TEM analysis finds the catalysts are highly dispersed materials.
- Catalysts favor the direct desulfurization pathway.

CoMoW sulfide nanocatalysts for the HDS of DBT from novel ammonium and alkyltrimethylammonium-thiomolybdate-thiotungstate-cobaltate (II) precursors

Y. Espinoza-Armenta[1], J. Cruz-Reyes[1], F. Paraguay-Delgado[2], M. Del Valle[1], G. Alonso[3], S. Fuentes, and R. Romero-Rivera[1*]
1) Facultad de Ciencias Químicas e Ingeniería, Universidad Autónoma de Baja California, Ave. Universidad 14418, Mesa de Otay, Tijuana, C.P. 22390, B.C., Mexico.
2) Depto. De Materiales Nanoestructurados, Centro de Investigación en Materiales Avanzados, S.C., Miguel de Cervantes 120, Chihuahua, Chih. CP. 31109, Mexico.
3) Centro de Nanociencias y Nanotecnología, Universidad Nacional Autónoma de México, Km 107 Carretera Tijuana-Ensenada, C. P. 22860, Ensenada, B.C., Mexico.

ABSTRACT

Five unsupported, highly active CoMoW trimetallic nanocatalysts were obtained by in situ decomposition form five novel precursors: $(NH_4)_2[Co(MoS_4)(WS_4)]$ and $(RN(CH_3)_3)_2[(MoS_4)(WS_4)]$ (where R=dodecyl, tetradecyl, cetyl and octadecyl), during the HDS of DBT. The catalyst labeled CoMoWS-C14, derived from the precursor containing the tetradecyl group, exhibits the highest catalytic activity (k =421x10^{-7}mol/g.s) . N_2 adsorption-desorption shows that the CoMoW catalysts are mesoporous materials with characteristic Type IV isotherms, having surface areas of 11-340 m^2/g. Elemental analysis by X-ray energy dispersive spectroscopy (EDS) working at STEM mode finds high concentrations of carbon ($3.7 \leq C/Mo \leq 11.3$ and $2.7 \leq C/W \leq 9$) in all the catalysts except CoMoWS, where carbon was not detected. The XRD patterns show that the catalysts are highly dispersed (less so for the CoMoWS) given the absence of the (002) reflection, along with broad and low intensity (101) and (110) reflections. High dispersion is also supported by the STEM micrographs showing unstacked layers. The selectivity of the reaction for all catalysts favors the direct desulfurization pathway. The surface area and high catalytic activity do not show direct correlation with the length of the hydrocarbon chains of the precursors.

Keywords: Molybdenum disulfide, HDS of DBT, tetraalkylammonium thiomolybdates, trimetallic catalyst

*Corresponding author
E-mail: dr.raulromero56@gmail.com
Phone: (664) 6822790

1. Introduction

The use of transition metal sulfide (TMS) catalysts in oil refinery hydrotreating has helped reduce the toxic SOx and NOx atmospheric emissions from internal combustion engines for several decades. Hydrotreating involves a variety of catalytic reactions, among them, hydrodesulfurization (HDS), hydrodenitrogenation (HDN), hydrodeoxygenation (HDO), and hydrogenation [1-4].

Typically the hydrotreating process is performed over alumina-supported catalysts based on molybdenum and tungsten sulfide, promoted with Co or Ni [5-7].

These materials are normally produced by sulfidation of the corresponding metal oxides. However, it is well known that incomplete sulfidation due to a strong interaction between metal and support results in a non-optimal hydrotreating activity [8].

Unsupported sulfide catalysts have been synthesized by different methods, including sulfidation of coprecipitated oxides [7, 9] comaceration [10-12], homogeneous sulfide precipitation [13], ceramic method [14], impregnated thiosalt decomposition [15], hydrothermal and solvothermal processes [16-20]. The structures and catalytic properties of the materials obtained by these methods strongly depend on their preparation and treatment conditions [12, 19, 21]. The thiosalt decomposition method is simple and reproducible and has been used in the preparation of binary and ternary sulfides with controlled stoichiometry, a wide range of specific surface area and improved catalytic activity [3, 22, 23].

Recently, the development of the NEBULA catalysts, with a HDS activity three times greater than conventional industrial catalysts, has renewed the interest in research focusing on unsupported trimetallic catalytic systems [24]. Nanostructured TMS such as MoS_2 -- with their high surface to volume ratio -- are also improving HDS performance over conventional catalysts [25-27].

This work reports the properties of new unsupported CoMoW sulfide catalysts obtained by *in situ* decomposition of novel ammonium and alkyltrimethylammonium-thiomolybdate-thiotungstate-cobaltate (II) precursors having lauryl (dodecyl, C_{12}), myristil (tetradecyl, C_{14}), cetyl (hexadecyl, C_{16}), and stearyl (octadecyl, C_{18}) as alkyl groups, respectively. These new precursors were prepared by reacting equimolar amounts (1:1:1) of the corresponding ammonium thiomolybdate, ammonium thiotungstate, alkyltrimethylammonium thiomolybdate, alkyltrimethylammonium thiotungstate, and $Co(NO_3)_2$. The catalytic activity of the catalysts was tested in the HDS of dibenzothiophene (DBT).

2. Experimental

2.1 Preparation of ammonium thiomolybdate (ATM)

Ammonium thiomolybdate, $(NH_4)_2MoS_4$, was prepared by bubbling hydrogen sulfide gas (H_2S) for 60 min in an aqueous solution of ammonium heptamolybdate, $(NH_4)_6Mo_7O_{24}$, and NH_4OH. After this process, red crystals were formed [28]. The resulting ATM was separated by vacuum filtration, washed with isopropyl alcohol, then dried at room temperature, and kept under N_2 atmosphere.

2.2 Preparation of ammonium thiotungstate (ATT)

Ammoniun thiotungstate $(NH_4)_2WS_4$ was prepared according to the method described by Ramanathan and Weller [29] which requires adding ammonium metatungstate, NH_4OH, H_2S and water, then heating at 60°C for 4 h to produce a dark yellow crystalline precipitate. The resulting ATT was separated by vacuum filtration, washed with isopropyl alcohol, then dried at room temperature, and kept under N_2 atmosphere.

2.3 Preparation of dodecyltrimethyl, tetradecyltrimethyl, hexadecyltrimethyl and octadecyltrimethyl-ammonium thiomolybdates

The alkyltrimethylammonium thiomolybdates were prepared according to the method reported by Romero et al [30], which requires freshly prepared ATM (1.62 g, 6.22 mmol) dissolved in water (50 mL) with stirring. An aqueous solution (12.44 mmol in 50 mL water) of alkyltrimethylammonium chloride, $R(CH_3)_3NBr$ (where R = dodecyl, tetradecyl, and octadecyl) or $R(CH_3)_3NCl$ (where R = hexadecyl) was then added and the mixture stirred for 1 h at room temperature. The resulting precipitate was separated by vacuum filtration, washed first with cold water and then with isopropyl alcohol. Each solid was dried at room temperature and kept under N_2 atmosphere.

2.4 Preparation of dodecyltrimethyl, tetradecyltrimethyl, hexadecyltrimethyl and octadecyltrimethyl-ammonium thiotungstates

Each alkyltrimethylammonium thiotungstate salt was prepared in a procedure analogous to the synthesis of the corresponding alkyltrimethylammonium-thiomolybdate [30]. Thus, freshly prepared ATT (2.17g, 6.25 mmol) was dissolved in water (50 mL) with stirring, then an aqueous solution (12.50 mmol in 50 mL water) of alkyltrimethylammonium bromide, $R\text{-}N(CH_3)_3Br$ (where R= dodecyl, tetradecyl, and octadecyl) or $R\text{-}N(CH_3)_3Cl$ (where R= hexadecyl) was added and the mixture stirred for 1 h at room temperature. The resulting precipitate was isolated by vacuum filtration, washed first with cold water and then with isopropyl alcohol. The solid was dried at room temperature and kept under N_2 atmosphere.

2.5 Synthesis of $(NH_4)_2[Co(MoS_4)(WS_4)]$ precursor.

Building on a procedure used by Müller et al [31-33], ATM (0.260 g, 1 mmol) was dissolved in 100 mL of a $CH_3CN{:}CH_3OH$ (2:3) solvent mixture, at room temperature. Then ATT (0.350 g, 1 mmol) dissolved in 90 mL of a $CH_3CN{:}CH_3OH$ (1:1) solvent mixture was added to this solution, at room temperature. Under N_2 atmosphere, the thiometallate mixture was added dropwise to $Co(NO_3)_2{\cdot}6H_2O$ (0.291 g, 1 mmol) dissolved in 10 mL of a $CH_3CN{:}CH_3OH$ (1:1) solvent mixture and acidified with acetic acid (1 mL), immediately forming a dark brown precipitate. Once the addition of the thiometallates was completed, the reaction mixture was stirred for 1 h at 0 °C. The resulting precipitate, labeled as CoMoWP, was filtered, washed with isopropyl alcohol, then air dried, and kept under N_2 atmosphere.

2.6. Preparation of $[R\text{-}N(CH_3)_3]_2[Co(MoS_4)(WS_4)]$ precursors

Following the procedure described in Section 2.5, dodecyltrimethylammonium thiomolybdate (0.681 g, 1.0 mmol) was dissolved in acetonitrile (30 mL), and added to a solution of dodecyltrimethylammonium thiotungstate (0.769 g, 1.0 mmol) in acetonitrile (20 mL), at room temperature. This thiometallate solution mix was then added dropwise at 0 ºC and under N_2 atmosphere to $Co(NO_3)_2{\cdot}6H_2O$ (0.291 g, 1.0 mmol) dissolved in acetonitrile (10 mL), then acidified with acetic acid (1 mL); a dark brown precipitate was produced immediately. Once the addition of the thiometallates was completed, the reaction mixture was stirred for one hour. The resulting precipitate, dodecyltrimethylammonium thiomolybdatethiotungstate cobaltate (II), labeled CoMoWP-C12, was filtered, washed with isopropyl alcohol, then air-dried, and kept under N_2 atmosphere.

The described procedure for the preparation of CoMoWP-C12 was used for the synthesis of the CoMoWP-C14, CoMoWP-C16 and CoMoWP-C18 precursors (where C14, C16 and C18 are the long chain alkyl groups of the ammonium ion), after modifying with acetonitrile:methanol solvents and increasing the temperature at which the thiometallate solution mix is prepared (equation 1), as described in Table 1.

$$[RN(CH_3)_3]_2MoS_4 + [RN(CH_3)_3]_2WS_4 + Co(NO_3)_2 \xrightarrow[N_2,\ 0\ ^{\circ}C,\ 1\ h]{CH_3CN:CH_3OH}$$

$$\longrightarrow (RN(CH_3)_3)_2[Co(MoS_4)(WS_4)] + 2\ RN(CH_3)_3NO_3 \qquad (1)$$

where R= dodecyl, tetradecyl, hexadecyl and octadecyl

Table 1. Reaction conditions for the preparation of CoMoWP-C_n trimetallic precursors

Precursor	T (ºC)	$[RN(CH_3)_3]_2$ MoS_4		$[RN(CH_3)_3]_2$ WS_4	
		w(g)	$CH_3CN:CH_3OH$ / mL	w(g)	$CH_3CN:CH_3OH$ / mL
CoMoWP-C12	25	0.681	1:0 / 30	0.769	1:0 / 20
CoMoWP-C14	25	0.737	1:1 / 70	0.825	1:1 / 50
CoMoWP-C16	50	0.793	7:3 / 100	0.881	1:1 / 50
CoMoWP-C18	60	0.849	9:1 / 50	0.937	9:1 / 50

2.7 Characterization of trimetallic catalysts after HDS Reaction

Specific surface areas were measured with a Quantachrome AUTOSORB-1 by N_2 adsorption at 77 K using the BET isotherm and a sample mass of 0.2 – 0.3 g. Samples were degassed under flowing argon at 473 K for 2 h before N_2 adsorption. The pore size distribution was obtained from the desorption data, following the BJH method. The mean standard deviation for the surface area measurements was about 2%.

The X-ray diffractograms for the prepared samples were obtained with a Philips X'Pert analytical diffractometer for powder samples using Cu Kα radiation. Their phases were identified with reference to the data base from the International Centre for Diffraction Data.

A Jeol JSM5800 LV scanning electron microscope was used to perform morphological analysis. Several zones were analyzed at different magnifications in order to recognize the prevalent features. Scanning Transmission electron microscopy micrographs and elemental analysis were done on Cs probe corrected Jeol JEM-2200FS analytical electron microscope operated at 200 kV. All images were recorded and evaluated (including Fourier analyses) with the Digital Micrograph (Gatan) software.

2.8 Catalytic activity and selectivity

The HDS of DBT was tested in a high pressure 300 mL Parr reactor by placing 4.4 g DBT, 100 mL of decalin and 100 mg of the trimetallic precursor. The reactor was purged of residual air, pressurized with H_2 to 3.1 MPa (450 psi) and then heated to the reaction temperature of 623 K in about 10 min. A stirring rate of 600 rpm was used. The progress of the reaction was monitored by gas chromatography in a HP 6890 gas chromatograph collecting samples every 20 min during the first hour, then every 30 min for the next four hours. Decrease of reaction mixture volume due to sampling was less than 5% of total volume. The identity of the reaction products was confirmed by mass spectrometry in a Agilent 6890 GC-MS, using a HP-5MS capillary column (30m X 0.25 mm X 0.25 μm).

Catalytic activity was expressed in terms of percentage conversion of DBT vs reaction time, and from this data the reaction rate constant, k', was calculated for each catalyst using the integrated form of the first order rate law (equation 2).

$$- \ln (1-X) = k't \quad (2)$$

where X is the DBT conversion fraction and t is the reaction time in minutes. A plot of [-ln (1-X)] vs time, optimized by linear regression, yields the value of k' as the slope of the plot. The specific rate constant, k , for the catalyst was then calculated by equation 3

$$k=k'\left(n_{DBT}\right)\left(\frac{1}{60}\right)\left(\frac{1}{w_{cat}}\right)=\left[mol/g.s\right] \quad (3)$$

where n_{DBT} is the initial amount of DBT in moles and w_{cat} is the weight of the recovered catalyst in grams. The mean standard deviation for catalytic measurements is about 2.5%.

The HDS of DBT yields biphenyl (BP) through the direct desulfurization pathway (DDS), and cyclohexylbenzene (CHB) and tetrahydrodibenzothiophene (THDBT) through the hydrogenation pathway (HYD). Since these two pathways are parallel [22], the selectivity (HYD)/(DDS) was approximately calculated by the equation 4:

$$HYD\big/DDS = \left\{\left[CHB\right]+\left[THDBT\right]\right\}\big/\left[BP\right] \quad (4)$$

3. Results and discussion

3.1 Elemental analysis

The elemental analysis of the in situ-prepared sulfide catalysts was determined by EDS and results are reported in Table 2. The Co:Mo:W atomic ratios, for all the materials differ from the nominal 1:1:1 stoichiometry values, with a S/Mo ratio between 3.5 and 5.7 Considerable amounts of carbon (3.6≤C/Mo≤11.3) were also found for all catalysts except for the CoMoWS, greater than those reported for another trimetallic catalyst [34]. The presence of carbon is attributed to the decomposition of the aliphatic chains of the tetraalkylammonium thiosalts (precursors), as suggested by other authors [34-37]. Besides surface carbon, a sulfur carbide phase could also form -- where the sulfur atoms are replaced by carbon atoms -- as observed in previous studies [38-40].

Table 2. Specific surface areas, total pore volume and elemental analysis determined by STEM for trimetallic catalysts CoMoWS-Cn.

Catalyst	Surface area (m^2/g)	Total pore volume (cm^3/g)	Composition
CoMoWS	12	0.037	$Co_{0.9}MoW_{0.9}S_{3.5}$
CoMoWS-C12	213	0.053	$Co_{0.8}MoW_{1.5}S_{5.7}C_{11.3}$
CoMoWS-C14	73	0.052	$Co_{0.9}MoW_{1.4}S_{4.2}C_{3.6}$
CoMoWS-C16	340	0.053	$Co_{0.9}MoW_{1.3}S_{5.0}C_{5.0}$
CoMoWS-C18	277	0.047	$Co_{0.8}MoW_{0.9}S_{3.7}C_{8.4}$

3.2 Textural properties

The specific surface areas and total pore volume values of trimetallic catalysts CoMoWS-Cn are reported in Table 2. Surface areas are between 12 and 340 m^2/g, mostly greater than the 11 – 52 m^2/g reported by Huirache, et al [34].

The average total pore volume is around 0.050 cm^3/g. Neither surface areas nor total pore volumes correlate with the size of the precursor's alkyl group. Average pore diameters are in the range 24-34 Å. The adsorption isotherms are shown in Fig. 1. All catalysts present a Type IV isotherm with desorption curves characteristic of mesoporous materials.

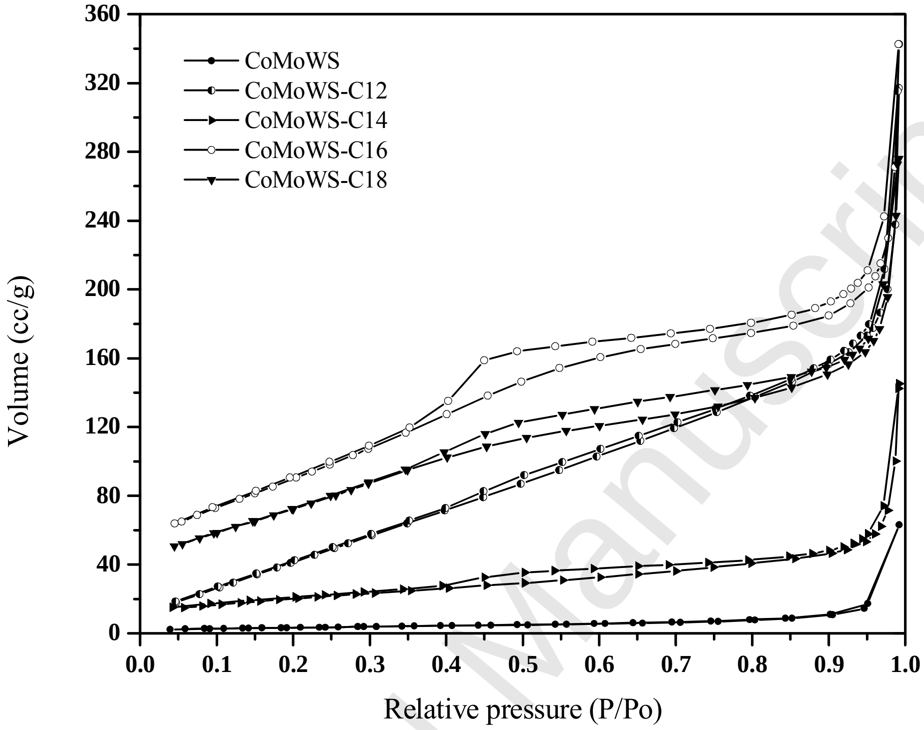

Fig. 1. N_2 adsorption-desorption isotherms of the trimetallic catalysts CoMoWS-Cn

The CoMoWS catalyst has a very narrow hysteresis loop and thus scarcely contributes to the porosity of the material, as evidenced by its surface area (Table 2), which is the lowest in the series. The CoMoWS-C12 catalyst also behaves like a poorly developed porous system, although not as pronounced as CoMoWS, which is consistent with the presence of a lower amount of carbon. The CoMoWS-C14, CoMoWS-C16 and CoMoWS-C18 catalysts have better developed porous systems, attributed to the precursor’s carbon content.

The hysteresis loop of CoMoWS, CoMoWS-C12, CoMoWS-C14 and CoMoWS-C18 is closer to the H3 type characteristic of slit-like pores or spaces formed for plate-like particles. The CoMoWS-C16 exhibits a hysteresis loop closer to the H2 type, associated with so called ink-bottle pores, composed of a cylindrical pore closed at one end and with a narrow neck at the other.

Save for the CoMoWS material, which is scarcely porous, all catalysts are found been mostly mesoporous, with average pore diameters in the range of 14-42 Å.

3.3 X-ray diffraction

The XRD patterns for the trimetallic catalysts CoMoWS-Cn are shown in Fig 2. For the CoMoWS, produced from a precursor that does not contain an aliphatic chain, several broad peaks are observed, with 2θ values at 12.94° (002), 33.79° (101) and 58.67° (110). The pattern is very similar to that of the hexagonal phases of 2H-MoS_2 and 2H-WS_2 (JCPDS-ICDD 37-1492, 8-0237). The broad peaks are characteristic of poorly crystalline materials, such as molybdenum sulfide derived from the decomposition of thiosalts [41].

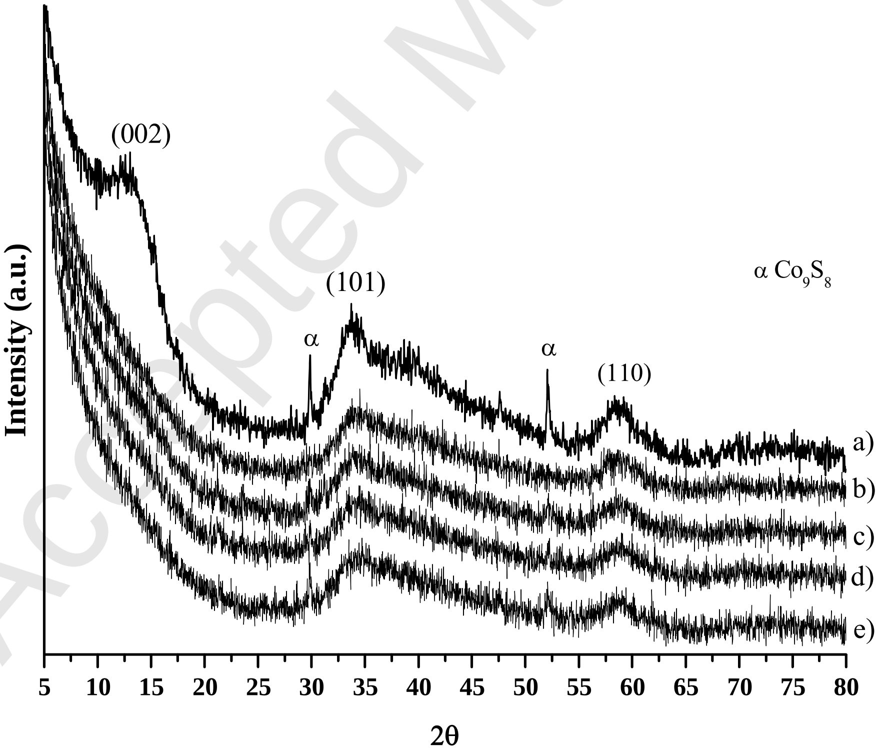

Fig. 2. XRD patterns of trimetallic catalysts CoMoWS-Cn:
a) CoMoWS, b) CoMoWS-C12, c) CoMoWS-C14,
d) CoMoWS-C16 and e) CoMoWS-C18

The low intensity (002) reflection implies a low number of stacking layers in the “c” direction of the catalyst particles. Moreover, narrow peaks at $2\theta = 29.89°$ (311) and 52.13° (440) which are clearly observed in CoMoWS, are attributed to crystalline cobalt sulfide phase Co_9S_8 (JCPDS-ICDD 2-1459).

In the diffraction patterns of the CoMoWS-C12, CoMoWS-C14, CoMoWS-C16 and CoMoWS-C18 derived from precursors that contain aliphatic chains of 12, 14, 16 and 18 carbons, respectively, the (002) reflection does not appear, suggesting they are highly dispersed or exfoliated materials [42, 43]. This dispersion could be attributed to the catalyst’s carbon content derived from the decomposition of the precursor’s aliphatic chain and the solvent (decalin). An analogous behavior has been reported for other MoS_2 and WS_2 systems where the carbon is considered to be the dispersing agent [44, 45]. The destacking effect of the (002) reflection has also been observed in the unsupported trimetallic sulfide system reported by Nava et al. [5], who find a low dispersion of the (002) reflection.

All catalysts in the series present a couple of very low-intensity broad peaks, at around $2\theta = 34°$ and 58°, corresponding to the (101) and (110) reflections of MoS_2 and WS_2, which are associated with materials of very low crystallinity. In contrast to previous studies [46, 47] where binary systems exhibited well-defined cobalt sulfide diffraction patterns, peaks belonging to the CoS or Co_9S_8 phases are barely observed, which suggest that the cobalt content is highly dispersed.

3.4 Transmission electron microscopy

Bright field STEM micrographs of the resulting catalysts (Fig. 3) show nearly spherical-shaped nanoparticles (<100 nm, according to the IUPAC classification), forming clusters of an average particle size (APS) between 53 and100 nm, as determined using the Gatan Digital Micrograph software.

Images at higher magnification of these trimetallic catalysts CoMoWS-Cn are shown in Fig. 4. These images are similar to that reported for a NiMoW unsupported ex-situ catalyst [48], showing highly disorganized curved fringes with only a few layers, as is also seen in the MoS_2/WS_2 poorly crystalline materials [37, 49]. Some bending of the layers is observed, which is characteristically due to the structural carbon content of the catalysts [44, 50].

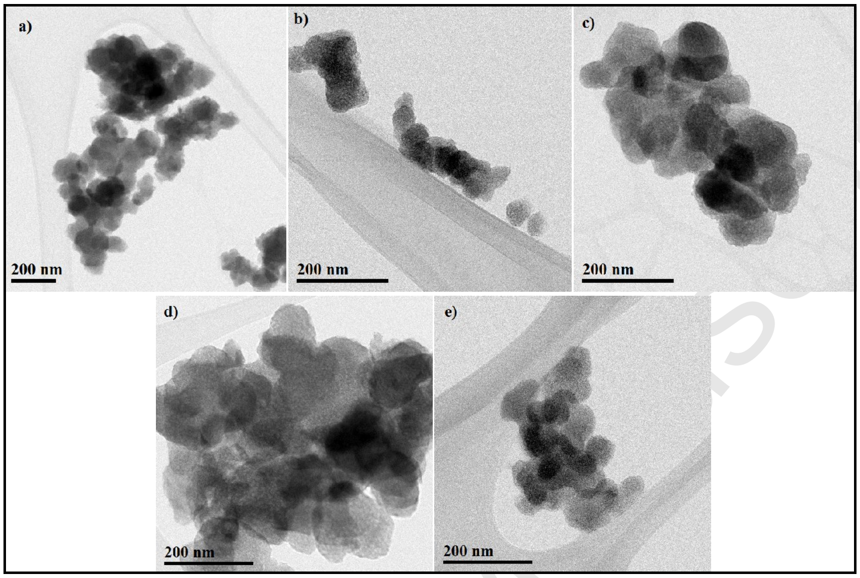

Fig. 3. STEM micrographs showing clusters of catalyst nanoparticles for:
a) CoMoWS, b) CoMoWS-C12, c) CoMoWS-C14, d) CoMoWS-C16,
e) CoMoWS-C18

Table 3. Average particle size for the CoMoWS-Cn catalysts

CoMoWS-Cn	APS (nm)	σ
CoMoWS	100	17
CoMoWS-C12	66	17
CoMoWS-C14	70	11
CoMoWS-C16	84	15
CoMoWS-C18	53	9

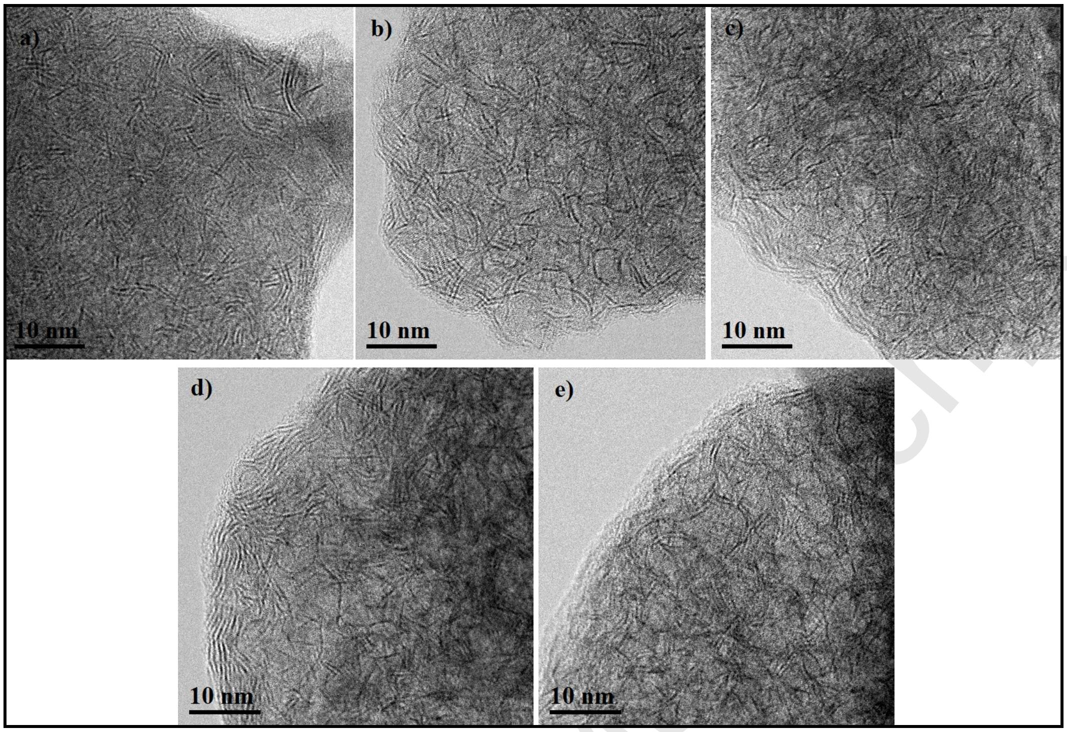

Fig. 4. TEM micrographs of the trimetallic catalysts CoMoWS-Cn:
a) CoMoWS, b) CoMoWS-C12, c) CoMoWS-C14,
d) CoMoWS-C16 and e) CoMoWS-C18.

3.5 Scanning electron microscopy

The morphology of the trimetallic catalysts CoMoWS-Cn is reported in Fig. 5. In general, these images show porous materials with irregular agglomerated particles and small cavities observed, which may result from the decomposition of the precursor's alkyl chains during the HDS of DBT, as discussed by Huirache et al. [34].

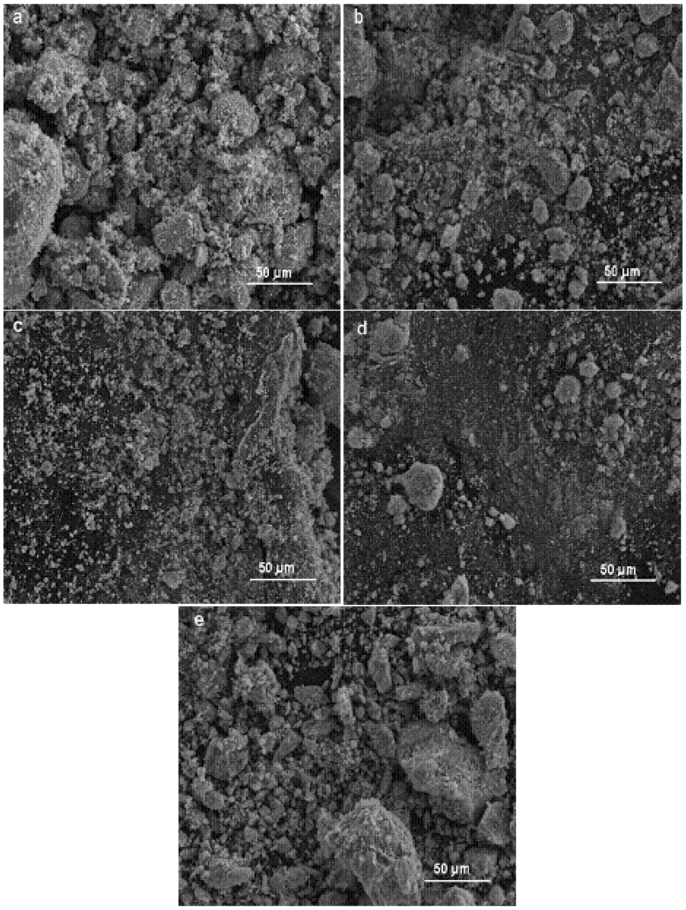

Fig. 5. SEM micrographs of the trimetallic catalysts CoMoWS-Cn:
a) CoMoWS, b) CoMoWS-C12, c) CoMoWS-C14
d) CoMoWS-C16 and e) CoMoWS-C18.

3.6 Catalytic activity and selectivity

The results of the catalytic test for the trimetallic catalysts CoMoWS, CoMoWS-C12, CoMoWS-C14, CoMoWS-C16 and CoMoWS-C18 are reported in the Table 4. The analysis of the kinetic data finds that the reaction of HDS of DBT closely follows a first order model during the first 5 h reaction time.

According to the GC analysis, the HDS of DBT yields mainly biphenyl (BP) through the direct desulfurization (DDS) pathway, and cyclohexylbenzene (CHB) and tetrahydrodibenzothiophene (THDBT) through the hydrogenation (HYD) pathway.

Cyclohexylcyclopentylmethane (CHCPM) and dicyclohexyl (DCH) can also be detected in the HYD pathway.

Table 4. Gas chromatography analysis* of HDS reaction products, HYD/DDS selectivity and kinetic data for trimetallic catalysts CoMoWS-Cn

Catalyst	CHCPM (%)	DCH (%)	CHB (%)	BP (%)	THDBT (%)	DBT (%)	Conversion DBT (%)	$\frac{[HYD]}{[DDS]}$	k x10^7 (mol/g.s)
CoMoWS	1.2	0.6	10.8	22.8	4.8	59.8	40.2	0.7	164
CoMoWS-C12	1.3	0.6	8.1	28.2	4.8	57.0	43.0	0.5	172
CoMoWS-C14	1.5	4.1	16.0	51.3	2.0	25.1	74.9	0.4	421
CoMoWS-C16	1.7	1.2	17.5	44.4	2.4	32.7	67.3	0.4	377
CoMoWS-C18	1.9	1.0	14.1	43.4	2.8	36.6	63.4	0.4	235

* After 5h of reaction

The experimental selectivity of all the catalysts favors DDS (HYD/DDS < 1) and it is mostly independent of the carbon content of the precursor. The highest DBT conversion was attained with the CoMoWS-C14 catalyst, resulting from the in situ decomposition of the CoMoWP-C14 precursor.

According to Table 4, the reference catalyst with no carbon (CoMoWS) has the lowest specific rate constant, k = 164×10^{-7} mol/g·s. The specific rate constant increases with the size of the alkyl groups of the precursors, resulting in a maximum k value (421×10^{-7} mol/g·s) for the CoMoWS-C14 catalyst, after which the k value decreases. The increase in k value from CoMoWS to CoMoWS-C14, does not correlate with an analogous increase in surface area over the same catalysts. In fact, the surface area of the CoMoWS-C14 catalyst is considerably less (73 m^2/g) than any of the other catalysts derived from the hydrocarbon sources. Moreover, no direct relation is found between the surface area and the catalytic activity as is generally the case among anisotropic transition metal sulfides [1], and bimetallic sulfides [51].

The increase in catalytic activity, especially in the case of CoMoWS-C14, is attributed to the presence of a mix of CoMoS and CoWS phases at the border faces of the microcrystals [52], which result in a high dispersion of cobalt; another factor is the particular nanostructure of the catalysts, which includes the presence of curved layers in the catalyst due to structural carbon from the precursors, as described by several authors [39, 53, 54]. The resulting specific rate constants are one order of magnitude greater than those reported by Huirache et al [34], Gochi et al [55], and Olivas et al [35].

CONCLUSIONS

The in situ decomposition, during the HDS of DBT, of five novel trimetallic precursors, one of them $(NH_4)_2[(MoS_4)(WS_4)]$ and the rest of the type $(RN(CH_3))_2[Co(MoS_4)(WS_4)]$, yields the corresponding trimetallic CoMoW nanostructured catalysts.

Their N_2 adsorption-desorption isotherms are Type IV, characteristic of mesoporous materials, with high surface areas.

XRD and TEM analysis find them to be highly dispersed materials.

Catalytic activity is not influenced by the size of the n-alkyl group of the precursor, having the CoMoWS-C14 catalyst as the most active at $k = 421x\ 10^{-7}$ mol/g.s.

The increase in catalytic activity is attributed to the presence of a mixture of CoMoS and CoWS phases in the edges of the faces of the microcrystals, the dispersion of which increased due to the structural carbon derived from the precursors. Microcrystals with curved layers are also seen. The CoMoWS-C14 catalyst is a good candidate for the deep HDS of other sulfur-containing compounds in the oils process.

Acknowledgements

We gratefully acknowledge technical assistance of C. Ornelas, E. Torres and L. de la Torre at the National Nanotechnology Lab of CIMAV-Chihuahua, Mexico. Y. Espinoza express gratefully for doctoral scholarship from CONACYT. G. Alonso acknowledges funding from CONACyT Project 155388 and PAPIIT IN104714. J. Cruz-Reyes and M. Del Valle acknowledge the economic support of UABC (13° y 14° Convocatoria Interna de Apoyo a Proyectos de Investigación).

References

[1] O. Weisser, S. Landa (1973) Sulfide Catalysts: Their Properties and Applications. Pergamon Press, Oxford.

[2] P. Grange, Catal. Rev. Sci. Eng. 21 (1980) 135-181.

[3] M. Zdrazil, Catal. Today 3 (1988) 269-365.

[4] H. Topsoe, B.S Clausen, F.E Massoth, Hydrotreating Catalysis Science and Technology (Anderson JR, Boudart M, Eds.), Springer-Verlag, Germany (1996) Vol. 11.

[5] H. Nava, F. Pedraza, G. Alonso, Catal. Lett. 99 (2005) 65-71.

[6] T. Kabe, W. Qian, A. Ishihara, J. Catal. 149 (1994) 171-180.

[7] W. Qian, A. Ishihara, S. Ogawa, T. Kabe, J. Phys. Chem. 98 (1994) 907-911.

[8] R. Prins, Adv. Catal. 46 (2001) 399-464.

[9] K.C Pratt, J.V Sanders, N. Tamp, J. Catal. 66 (1980) 82-92.

[10] J.V Sanders, K.C Pratt, J. Catal. 67 (1981)331-347.

[11] G. Hagenbach, Ph. Courty, B. Delmon, J. Catal. 23 (1971) 295-300.

[12] H. Ishihara, T Itoh., Y. Hino, M. Nomura, P. Qi, T. Kabe, J. Catal. 140 (1993) 184 -189.

[13] G. Hagenbach, Ph. Courty, B. Delmon, J. Catal. 31 (1973) 264-273.

[14] R. Candia, B.J. Clausen, H. Topsoe, Bull. Soc. Chim. Belg. 90 (1981) 1225-1232.

[15] A.A. Al-Hilli, B.L. Evans, J. Crystal Growth 15 (1972) 93-101.

[16] Y.Y. Peng, Z.Y. Meng, C. Zhong, J. Lu , W.C. Yu, Z.P. Yang, Y.T. Qian, J. Solid State Chem. 159 (2002) 170-173.

[17] Y.Y. Peng, Z.Y. Meng, C. Zhong , J. Lu, W.C. Yu, Y.B. Jia, Y.T. Qian, Chem. Lett. 30 (2001) 772-773.

[18] W.J. Li, E.W. Shi, J.M. Ko, H. Ogino, T. Fukuda, J. Cryst. Growth 250 (2003) 418-422.

[19] E. Devers , P. Afanasiev, B. Jouguet, M. Vrinat, Catal. Lett. 82 (2002)13-17.

[20] N. Rueda, R. Bacaud, M. Vrinat, J. Catal. 169 (1997) 404-406.

[21] K.S. Liang, R.R. Chianelli, F.Z. Chien, S.C. Moss, J Non-Cryst Solids 79 (1986) 251-273.

[22] S. Fuentes, G. Diaz , F. Pedraza, H. Rojas, N. Rosas, J. Catal 113 (1988) 535-539.

[23] A.W. Naumann, A.S. Behan, U.S. Patent 4,243,554 (1981).

[24] S.L. Soled, S. Miseo, R. Krikak, H. Vroman , T.C. Ho, K.L. Riley, U.S. Patent 6,299,760 (2001)

[25] M.M. Mdleleni, T. Hyeon, K.S. Suslick, J. Am. Chem. Soc. 120 (1998) 6189-6190.

[26] Y. Iwata, K. Sato, T. Yoneda, Y. Miki, Y. Sugimoto, A. Nishijima, H. Shimada, Catal. Today 45 (1998) 353-359.

[27] G.A. Camacho-Bragado, J.L. Elechiguerra, A. Olivas, S. Fuentes, D. Galvan, M.J. Yacaman, J. Catal. 234 (2005) 182-190.

[28] G. Kruss, Justus Liebigs Ann. Chem. 225 (1884) 1-57.

[29] K. Ramanathan, W.S. Weller, J. Catal. 95 (1985) 249-259.

[30] R. Romero-Rivera, A.G. Camacho, M. Del Valle, G. Alonso, S. Fuentes, J. Cruz-Reyes, Top. Catal. 54 (2011) 561-567.

[31] A. Müller, E. Diemann, J. Chem. Soc. D (1971) 65a-65a.

[32] A. Müller, E. Diemann, H. Heinsen, Chem. Ber. 104 (1971) 975-980.

[33] A. Müller, M.C. Chakravorti, H. Dornfeld, Z. Natureforsch 30B (1975) 162-164.

[34] R. Huirache-Acuña, M.A. Albiter, C. Ornelas, F. Paraguay-Delgado, R. Martínez-Sánchez, G. Alonso-Núñez, App. Catal. A 308 (2006) 134-142.

[35] A. Olivas, D.H Galván, G. Alonso, S. Fuentes, App. Catal. A 352 (2009) 10-16.

[36] G. Alonso, M.H Siadati, G. Berhault, A. Aguilar, S. Fuentes, R.R Chianelli, Appl. Catal. A 263 (2004) 109-117.

[37] R. Romero-Rivera, G. Berhault, G. Alonso-Nuñez, M. Del Valle, F. Paraguay-Delgado, S. Fuentes, S. Salazar, A. Aguilar, J. Cruz-Reyes, Appl. Catal. A 433 (2012) 115-121.

[38] A) G. Alonso, M. Del Valle, J. Cruz, A. Licea Claverie, V. Petranovskii, S. Fuentes, Catal. Lett. 52 (1998) 55-61;

[39] G. Berhault, A. Mehta, A.C. Pavel, J. Yang, L. Rendon, M.J. Yacaman, L. Cota, A. Duarte, R.R. Chianelli, J. Catal. 198 (2001) 9-19;

[40] V. Schwartz, V. Texeira da Silva, S.T. Oyama, J. Mol. Cat. A 163 (2000) 251-268.

[41] K.S. Liang, R.R. Chianelli, F.Z. Chien, S.C. Moss, J. Non-Cryst. Solids 79 (1986) 251-273.

[42] M. Del Valle, J. Cruz-Reyes, M. Avalos-Borja, S. Fuentes, Catal. Lett. 54 (1998) 59-

63.

[43] P. Afanasiev, G.F. Xia, G. Berhault, B. Jouguet, M. Lacroix, Chem. Mater. 11 (1999) 3216-3219.

[44] S.P. Kelty, G. Berhault, R.R. Chianelli, Appl. Catal. A 322 (2007) 9-15.

[45] X. Jin, C. Ma, Y. Yi, Q. Zhang, J. Qiu, C. Liang, J. Phys. Chem. Solids 71 (2010) 642-646.

[46] R.W. Phyllips, A.A. Fote, J. Catal. 41 (1976) 168-172.

[47] S. Gobolos, Q. Wu, J. Ladriere, F. Delannay, B. Delmon, Bull. Soc. Chim. Belg. 93 (1984) 687-696.

[48] B.S. Zhang, Y.J. Yi, W. Zhang, C.H. Liang, D.S. Su, Mater. Charact.62 (2011) 684-690.

[49] R.R. Chianelli, E.B. Presstidge, T.A. Pecoraro, J.P. Deneufville, Science 203 (1979) 1105-1107.

[50] G. Berhault, L. Cota Araiza, A. Duarte Moller, A. Metha, R.R. Chianelli, Catal. Lett. 78 (2002) 81-90.

[51] R.R. Chianelli, G. Berhault, Catal. Today 53 (1999) 357-366.

[52] C. Wivel, R. Candia, B.S. Clausen, S. Morup, H.Topsoe, J. Catal. 68 (1981) 453-463.

[53] A. Nogueira, R. Znaiguia, D. Uzio, P. Afanasiev, G. Berhault, Appl. Catal. A 429 (2012) 92-105.

[54] W. Iwata, Y. Araki, K. Honna, Y.Miki, K. Sato, H. Shimada, Catal. Today 65 (2001) 335-341

[55] Y. Gochi, C. Ornelas, F. Paraguay, S. Fuentes, L. Alvarez, J.L.Rico, G. Alonso-Núñez G, Catal. Today 107 (2005) 531-536.

FIGURES

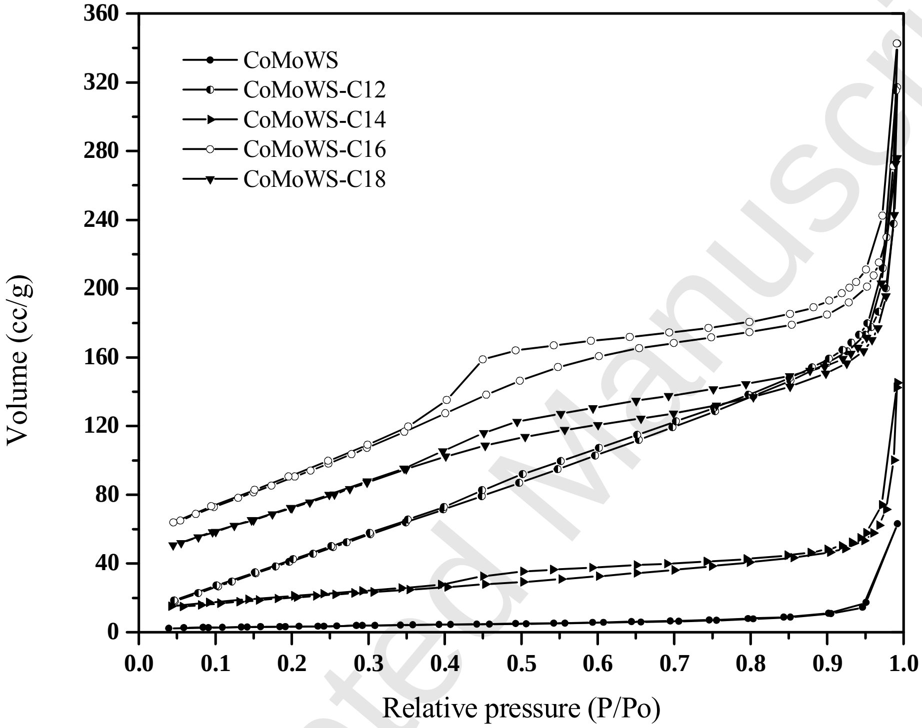

Y. Espinoza et al
Fig. 1

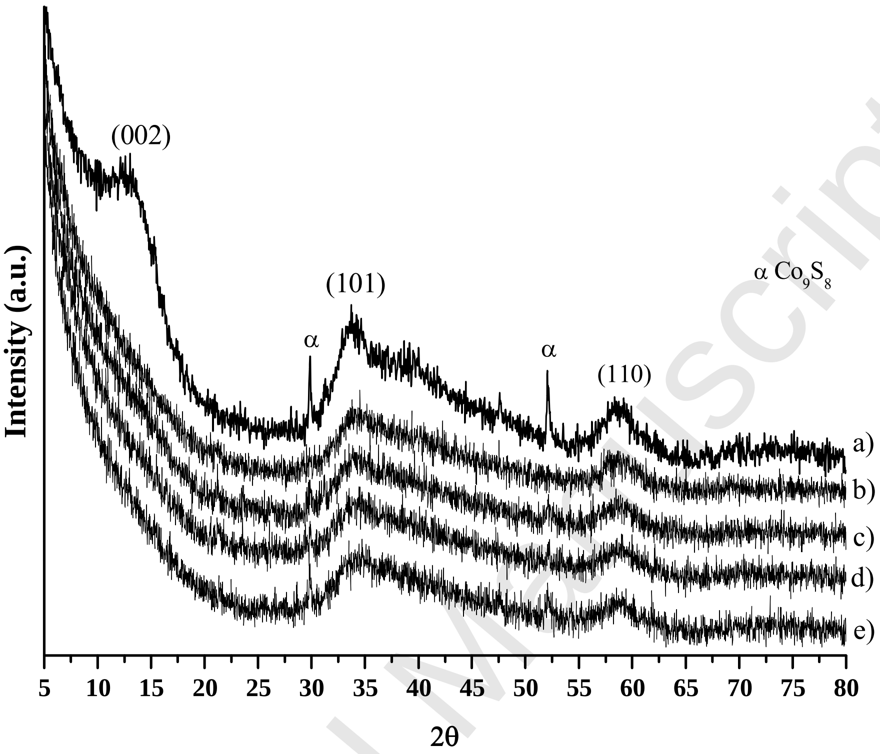

Y. Espinoza et al
Fig. 2

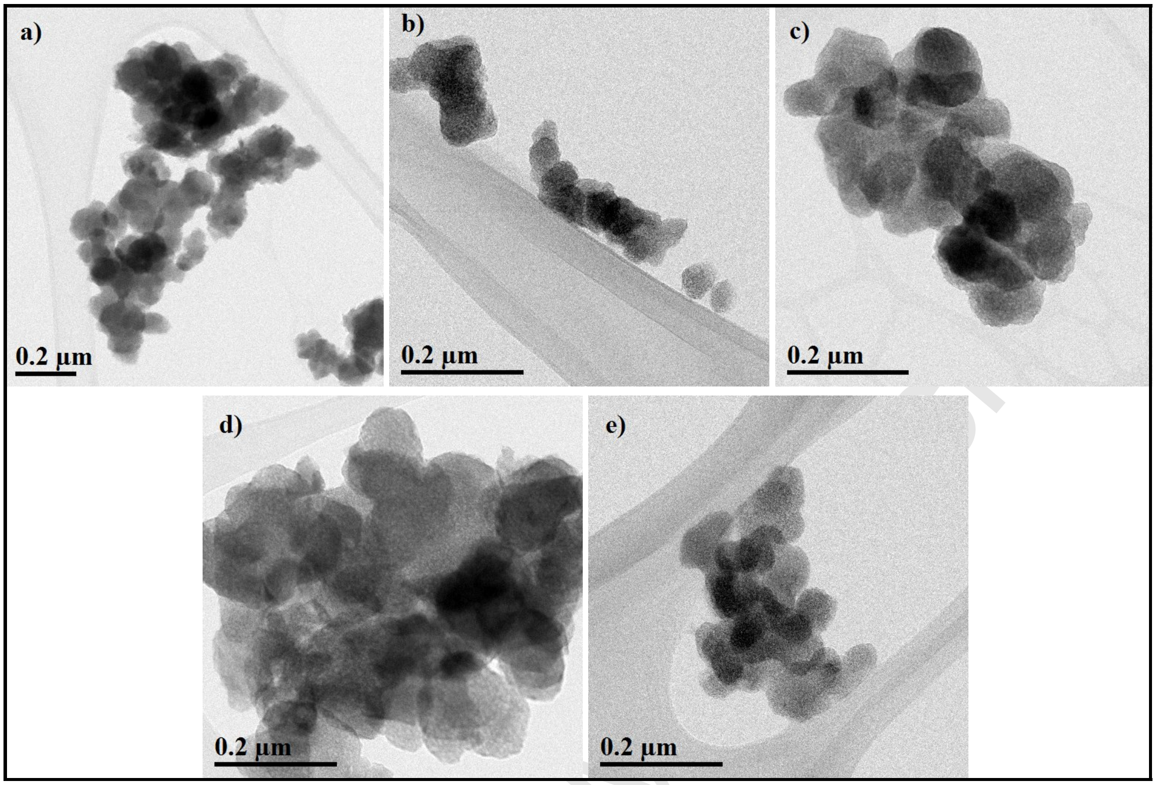

Y. Espinoza et al
Fig. 3

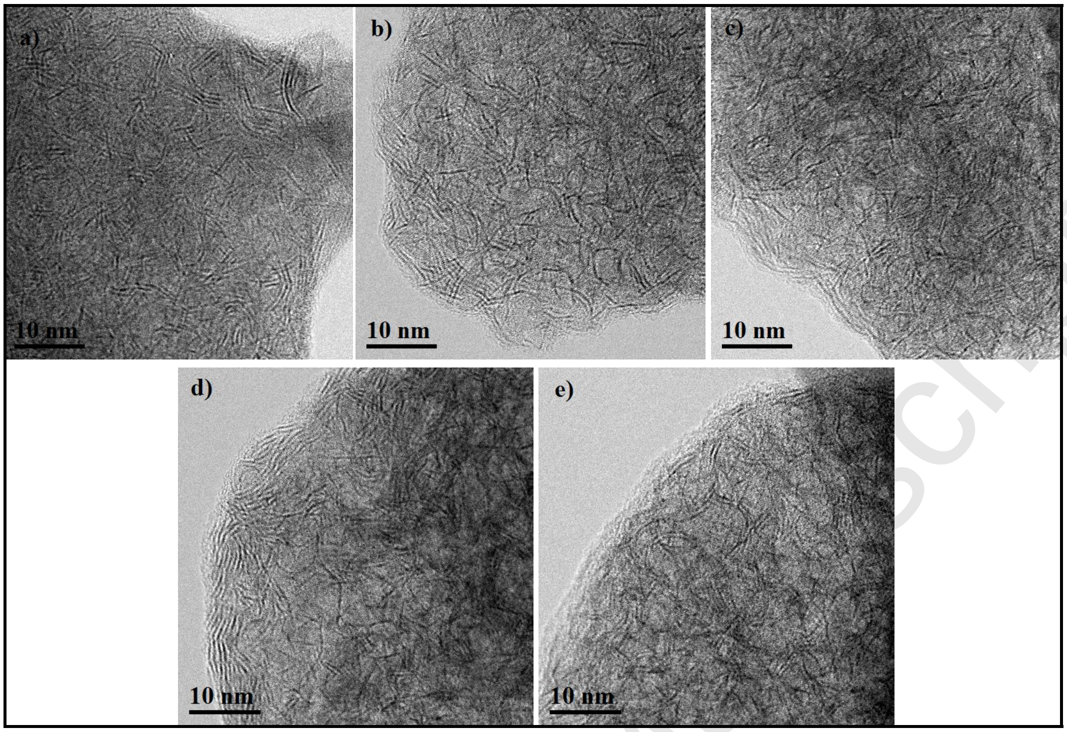

Y. Espinoza et al
Fig. 4

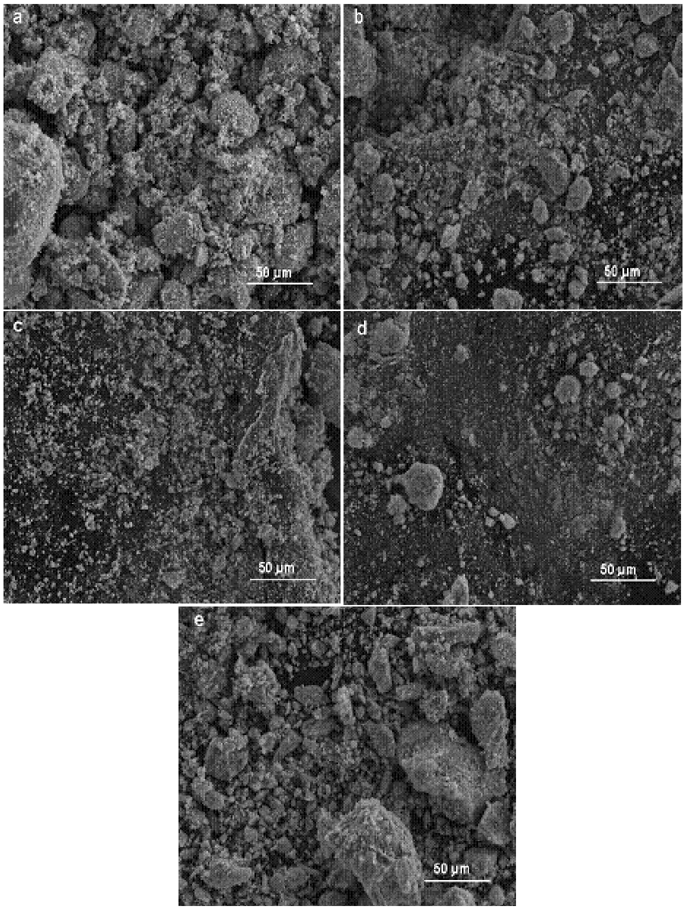

Y. Espinoza et al
Fig. 5

FIGURE CAPTIONS

Fig. 1. N_2 adsorption-desorption isotherms of the trimetallic catalysts CoMoWS-Cn

Fig. 2. XRD patterns of trimetallic catalysts CoMoWS-Cn:

b) CoMoWS, b) CoMoWS-C12, c) CoMoWS-C14,
d) CoMoWS-C16 and e) CoMoWS-C18

Fig. 3. TEM micrographs showing clusters of catalyst nanoparticles for:

b) CoMoWS, b) CoMoWS-C12, c) CoMoWS-C14, d) CoMoWS-C16,

e) CoMoWS-C18

Fig. 4. TEM micrographs of the trimetallic catalysts CoMoWS-Cn:

a) CoMoWS, b) CoMoWS-C12, c) CoMoWS-C14,
d) CoMoWS-C16 and e) CoMoWS-C18.

Fig. 5. SEM micrographs of the trimetallic catalysts CoMoWS-Cn:

a) CoMoWS, b) CoMoWS-C12, c) CoMoWS-C14
d) CoMoWS-C16 and e) CoMoWS-C18.